



CHORUS

This is the accepted manuscript made available via CHORUS. The article has been published as:

Pressure-tuned superconductivity and normal-state behavior in $\text{Ba}(\text{Fe}_{0.943}\text{Co}_{0.057})_2\text{As}_2$ near the antiferromagnetic boundary

W. Liu, Y. F. Wu, X. J. Li, S. L. Bud'ko, P. C. Canfield, C. Panagopoulos, P. G. Li, G. Mu, T. Hu, C. C. Almasan, and H. Xiao

Phys. Rev. B **97**, 144515 — Published 23 April 2018

DOI: [10.1103/PhysRevB.97.144515](https://doi.org/10.1103/PhysRevB.97.144515)

Pressure tuned superconductivity and normal state behavior in $\text{Ba}(\text{Fe}_{0.943}\text{Co}_{0.057})_2\text{As}_2$ near the antiferromagnetic boundary

W. Liu^{1,3}, Y. F. Wu², X. J. Li¹, S. L. Bud'ko⁴, P. C. Canfield⁴, C. Panagopoulos⁵, P. G. Li³, G. Mu², T. Hu^{2†}, C. C. Almasan⁶, and H. Xiao^{1*}

¹ Center for High Pressure Science and Technology Advanced Research, Beijing, 100094, China

² State Key Laboratory of Functional Materials for Informatics, Shanghai Institute of Microsystem and Information Technology, Chinese Academy of Sciences, 865 Changning Road, Shanghai 200050, China

³ Department of Physics, Zhejiang SCI-TECH University, Hangzhou, 310018 China

⁴ Ames Laboratory and Department of Physics and Astronomy, Iowa State University, Ames, Iowa 50011

⁵ Division of Physics and Applied Physics, School of Physical and Mathematical Sciences, Nanyang Technological University, 637371 Singapore and

⁶ Department of Physics, Kent State University, Kent, Ohio, 44242, USA

(Dated: April 11, 2018)

Superconductivity in iron pnictides is unconventional and pairing may be mediated by magnetic fluctuations in the Fe-sublattice. Pressure is a clean method to explore superconductivity in iron based superconductors by tuning the ground state continuously without introducing disorder. Here we present a systematic high pressure transport study in $\text{Ba}(\text{Fe}_{1-x}\text{Co}_x)_2\text{As}_2$ single crystals with $x = 0.057$, which is near the antiferromagnetic instability. Resistivity $\rho = \rho_0 + AT^n$ was studied under applied pressure up to 7.90 GPa. The parameter n approaches a minimum value of $n \approx 1$ at a critical pressure $P_c = 3.65$ GPa. Near P_c , the superconducting transition temperature T_c reaches a maximum value of 25.8 K. In addition, the superconducting diamagnetism at 2 K shows a sudden change around the same critical pressure. These results may be associated with a possible quantum critical point hidden inside the superconducting dome, near optimum T_c .

A. Introduction

Unconventional superconductivity observed in iron-based superconductors is in close proximity to an antiferromagnetically ordered state.¹ Superconductivity emerges as antiferromagnetism is suppressed by pressure or chemical doping,²⁻⁴ and the superconducting critical temperature T_c forms a dome shape. In the Ni-, Co-, P-, Rh- and Pd-doped BaFe_2As_2 system, the antiferromagnetic phase boundary crosses the superconducting dome near optimal doping.^{2,5-10} Hence, there is a region in the phase diagram where antiferromagnetism and superconductivity coexist. Neutron scattering measurements on $\text{Ba}(\text{Fe}_{1-x}\text{Ni}_x)_2\text{As}_2$ observed short range incommensurate antiferromagnetic order coexisting with superconductivity near optimal doping, where the first-order-like antiferromagnetism-to-superconductivity transition suggests the absence of a quantum critical point (QCP).⁶ Notably, it has been reported that the magnetic penetration depth in $\text{BaFe}_2(\text{As}_{1-x}\text{P}_x)_2$ shows a sharp peak at optimal doping, possibly due to quantum fluctuations associated with a QCP.⁷

In particular for $\text{Ba}(\text{Fe}_{1-x}\text{Co}_x)_2\text{As}_2$, the physical properties have been widely studied close to optimal doping and the antiferromagnetic phase boundary. Neutron diffraction measurements indicate Co doping rapidly suppresses antiferromagnetism, with the antiferromagnetic order vanishing at $x \approx 0.055$.¹¹ For $x = 0.06$, it is suggested that superconductivity coexists with a spin density wave (SDW).¹² For thin films of $\text{Ba}(\text{Fe}_{1-x}\text{Co}_x)_2\text{As}_2$, the exponent n in the temperature dependence of the resistivity is minimum namely, close to unity at $x \approx$

0.05 and $x \approx 0.07$ for MgO and CaF_2 substrate, respectively, which may be associated with an antiferromagnetic QCP.¹³ Furthermore, a sign change in the electronic-magnetic Gruneisen parameter is observed for $x = 0.055$ and $x = 0.065$, consistent with the expected behavior at a QCP.¹⁴ In addition, a critical concentration of $x_c \approx 0.065$ is determined from the analysis of $1/T_1T$ in NMR measurements.¹⁵ Considerably enhanced flux-flow resistivity ρ_{ff} was also detected for $x = 0.06$, perhaps due to enhancement of spin fluctuations near QCP.¹⁶ Thermopower (S) measurements reported a maximum S/T in proximity to the commensurate-to-incommensurate SDW transition for $x \approx 0.05$, close to the highest superconducting T_c .¹⁷ However, the superconducting magnetization appears nearly unchanged across the dome in $\text{Ba}(\text{Fe}_{1-x}\text{Co}_x)_2\text{As}_2$.²

Despite extensive studies in $\text{Ba}(\text{Fe}_{1-x}\text{Co}_x)_2\text{As}_2$ close to optimal doping, there had been no systematic study on how the normal state evolves across the antiferromagnetic phase boundary. Here we probe the phase diagram close to the antiferromagnetic boundary through measurements of resistivity and magnetization by tuning the applied pressure in a sample with $x = 0.057$. Normal state resistivity changes from non-Fermi liquid to Fermi liquid with increasing pressure. It shows almost linear temperature dependence at a critical pressure of $P = 3.65$ GPa, where T_c is maximum. In addition, the residual resistivity ρ_0 and the resistivity at T_c all change around the same critical pressure. From the magnetization data, the superconducting diamagnetism at 2 K shows a sudden change at a critical pressure of $P = 3.5$ GPa, in accordance with changes in resistivity. These results may be

78 due to a possible QCP at optimum T_c , similar to the case
79 of $\text{BaFe}_2(\text{As}_{1-x}\text{P}_x)_2$ ⁷ and hole doped cuprates.¹⁸

80 B. Experimental Details

81 Single crystals of $\text{Ba}(\text{Fe}_{1-x}\text{Co}_x)_2\text{As}_2$ with $x = 0.057$
82 were synthesized by a flux method.² Electrical resistivity
83 was measured using a Quantum Design Physical Property
84 Measurement System (PPMS). The electronic transport
85 properties were measured using four-probe electrical
86 conductivity in a diamond anvil cell made of CuBe
87 alloy. The diamond culet was 800 μm in diameter. Mag-
88 netic measurements were performed in a superconducting
89 quantum interference device (SQUID magnetometer).
90 Pressure was applied using a diamond anvil cell
91 made of CuBe alloy with the diamond anvil culet of
92 500 μm . In both cases, Daphne oil 7373 was used as
93 a pressure-transmitting medium. Above its solidification
94 at 2.2 GPa,¹⁹ non-hydrostaticity may develop and lead
95 to inhomogeneous pressure distribution inside the sam-
96 ple chamber. Pressure was calibrated by using the ruby
97 fluorescence shift at room temperature. For resistivity,
98 the superconducting transition temperature T_c is defined
99 as the temperature for the appearance of zero resistance
100 state (Fig. 1(b)); for magnetization, T_c is the tempera-
101 ture we observe a sharp drop in M (inset to Fig. 3(a)).

102 C. Results and Discussion

103 Figure 1 shows the temperature dependence of resis-
104 tivity for $\text{Ba}(\text{Fe}_{1-x}\text{Co}_x)_2\text{As}_2$ with $x = 0.057$ measured
105 at different applied pressures namely, $P = 0, 1.25, 2.69,$
106 $3.65, 5.26, 6.87$ and 7.90 GPa. The resistivity curve for
107 $P = 7.90$ GPa was shifted downward by 0.05 m Ω cm for
108 clarity. Note that the large decrease of ρ_{300K} with pres-
109 sure (inset to Fig. 1(b)) is very similar to the changes
110 occurring with Co doping in $\text{Ba}(\text{Fe}_{1-x}\text{Co}_x)_2\text{As}_2$.²⁰ By
111 comparing the data we find that an increase in doping
112 level by 1% is roughly equivalent to 1.2 GPa of pressure,
113 which is comparable with previous report.¹⁴

114 At low pressures, resistivity decreases with decreas-
115 ing temperature but shows an upturn just before enter-
116 ing the superconducting state. This upturn is due
117 to the structural (T_s) and SDW (T_{sdw}) phase transi-
118 tion, in agreement with earlier studies in underdoped
119 $\text{Ba}(\text{Fe}_{1-x}\text{Co}_x)_2\text{As}_2$.² Both T_s and T_{sdw} can be estimated
120 from the first derivative of the temperature dependent
121 resistivity curve (see inset to Fig. 1(a)).⁵ With further
122 increase in pressure, the upturn vanishes suggesting sup-
123 pression of the T_s and T_{sdw} . Similar changes with pres-
124 sure has been reported for $\text{Ba}(\text{Fe}_{1-x}\text{Co}_x)_2\text{As}_2$.²⁰⁻²² The
125 zero resistance transition temperature T_c (solid squares
126 in Fig. 2(a)) varies non-monotonically with increasing
127 pressure. For $P = 6.87$ GPa and above, we observe a
128 finite resistivity down to the lowest measured tempera-
129 ture. A similar dome shaped variation in T_c is observed

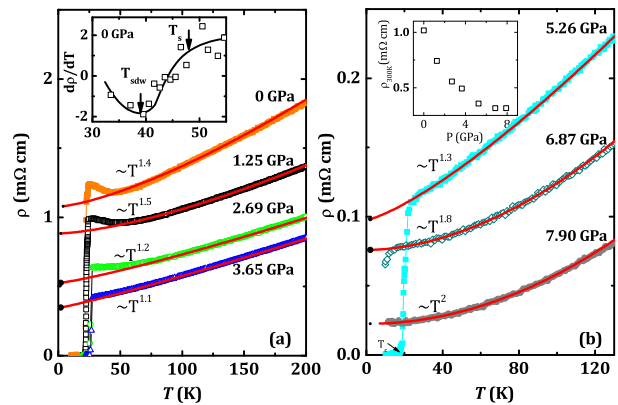


FIG. 1. (a)(b) Temperature T dependence of resistivity ρ under applied pressure $P = 1.25, 2.69, 3.65, 5.26, 6.87$ and 7.90 GPa. Symbols represent data and solid lines are fits using $\rho = \rho_0 + AT^n$. Note that the resistivity curve for $P = 7.90$ GPa was shifted downward by 0.05 m Ω cm for clarity. Inset to (a) shows the temperature dependence of $d\rho/dT$ at ambient pressure. Inset to (b) shows pressure dependence of resistivity at 300 K, ρ_{300K} .

130 in $\text{Ba}(\text{Fe}_{1-x}\text{Co}_x)_2\text{As}_2$ with Co doping.^{21,22}

131 We fit the resistivity curve under pressure using $\rho =$
132 $\rho_0 + AT^n$ (with fitting parameters ρ_0, n and A) as shown
133 in Fig. 1, where the symbols represent data points and
134 the solid lines are fits. The pressure dependence of $T_c,$
135 ρ_0, ρ at T_c and n obtained from Fig. 1 are summarized
136 in Fig. 2(a)-(c), respectively. Resistivity can be tuned
137 with pressure from a non-Fermi liquid (NFL) ($n = 1$) to
138 Fermi liquid (FL) ($n = 2$) behavior. Note that $n = 1.1$
139 at $P = 3.65$ GPa and increases with further increase in
140 pressure, reaching 2 at $P = 7.90$ GPa.

141 Interestingly, all parameters in Fig. 2 show a change
142 at $P_c \approx 3.5$ GPa. This is similar to the heavy fermion
143 superconductor CeCoIn_5 , where ρ_0 and n change at $P_c =$
144 1.6 GPa.²³ We ascribe the decrease in ρ_0 with increas-
145 ing pressure to a change in inelastic scattering.²³ The
146 pressure dependence of ρ at T_c shows a change in slope
147 at P_c , similar to the behavior of the normal state resis-
148 tivity ρ_n at T_c around optimal doping in chemically
149 tuned BaFe_2As_2 .¹² Similar change in n was also ob-
150 served in BaFe_2As_2 with Co doping, where the exponent
151 n is minimum namely, close to 1 at optimal doping.¹³
152 In $\text{BaFe}_2(\text{As}_{1-x}\text{P}_x)_2$, non-Fermi liquid behavior with n
153 close to unity is found around optimal doping $x = 0.3,$
154 with T_c maximum at the QCP.⁷ Similarly, linear resis-
155 tivity was observed for $\text{Ba}(\text{Fe}_{1-x}\text{Ni}_x)_2\text{As}_2$ with $x = 0.05$
156 for which T_c is maximum at a magnetic QCP.²⁴

157 The zero field cooled (ZFC) magnetization was mea-
158 sured in a run with increasing pressure for $P = 0.6, 1.2,$
159 $2.0, 2.7, 3.5, 4.3, 5.6, 6.4$ GPa. The resultant data are
160 plotted in Fig. 3(a). Since the sample used in the pres-
161 sure cell is too small to measure its mass, we show mag-
162 netization data in emu. Another piece of sample is used
163 to obtain the ambient pressure magnetization data (as
164 shown in the inset to Fig. 3(a)) to determine T_c at $P = 0.$

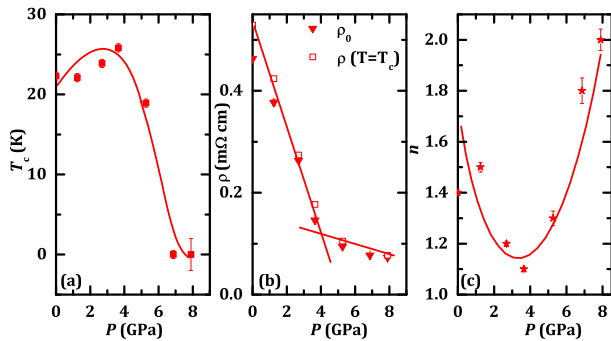


FIG. 2. Pressure dependence of (a) superconducting transition temperature T_c , (b) resistivity at the superconducting onset temperature $\rho(T = T_c)$ and residual resistivity ρ_0 , (c) exponent n .

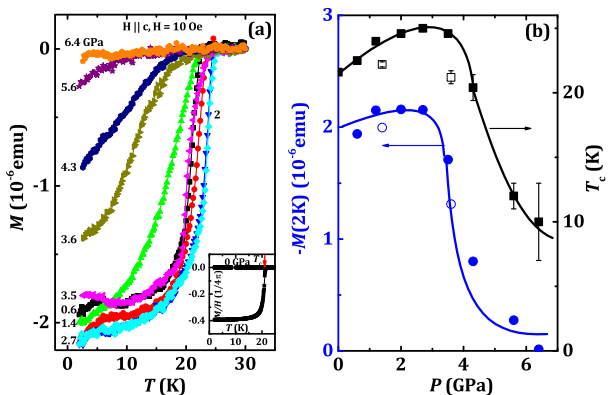


FIG. 3. (a) Temperature dependence of magnetization measured at $P = 0.6, 1.2, 2, 2.7, 3.5, 4.3, 5.6, 6.4$ GPa with increasing pressure and $3.6, 1.4$ GPa with decreasing pressure, in an applied magnetic field of 10 Oe. The inset shows magnetization data at ambient pressure for both zero field cooled (ZFC) and field cooled (FC) runs. (b) Pressure dependence of the superconducting transition temperature (squares) and the diamagnetic signal $M(2K)$ (circles). Solid and open symbols depict data for experiments performed with increasing and decreasing pressure, respectively.

The pressure dependence of T_c determined from magnetization measurements is plotted in Fig. 3(b), consistent with the T_c obtained from resistivity measurements (Fig. 2(a)).

We summarize the pressure dependence of the ZFC magnetization at $T = 2$ K, $M(2K)$ in Fig. 3(b). Note that the magnetization data at low temperatures was often used to estimate the superconducting volume fraction.^{25–27} In our case, it may not be accurate to estimate the volume fraction of superconductivity from magnetization since the superconducting transitions are broad and incomplete at high pressures and upon releasing the pressure. Nevertheless, it will give some hint to further understand the behavior of the superconducting state evolving across the antiferromagnetic phase boundary. Initially, M_{2K} slightly increases with pressure fol-

lowed by a sudden suppression at $P_c = 3.5$ GPa, then becoming negligible at high pressures. A similar pressure induced suppression in the superconducting volume was observed in the parent compound of BaFe_2As_2 and SrFe_2As_2 , where a dome like behavior of the pressure dependent superconducting volume is reported.²⁸ Also, for $\text{Sr}(\text{Fe}_{1-x}\text{Ni}_x)_2\text{As}_2$ and $\text{Ca}_{1-x}\text{LaFe}_2(\text{As}_{1-y}\text{P}_y)_2$, the superconducting volume shows a dome behavior with doping.^{25,27} In addition, a sudden suppression in the superconducting volume was observed in high- T_c cuprate $\text{La}_{2-x}\text{Sr}_x\text{CuO}_4$ at a critical doping level of around $x = 0.21$,²⁹ which is close to a QCP.³⁰ Thus, the suppression of the superconducting volume fraction above the critical pressure observed in present work could reflect a phase transition at P_c .

Note that in chemically doped (Co, Rh, Ni) BaFe_2As_2 at ambient pressure, there is no change in magnetization across the dome.^{2,5,9} Nevertheless, this difference may be due to different role played by pressure and chemical tuning. In fact, there is a pressure tuned QCP in pure CeCoIn_5 ,²³ while, there is no signatures of quantum critical behavior in Cd-doped CeCoIn_5 , due to the effect of disorder near a zero temperature magnetic instability.³¹ This suggests that tuning a system with disorder to a presumed magnetic QCP does not necessitate a quantum critical response.³¹

We also measured two magnetization curves under decompression, namely, for $P = 3.6$ and 1.4 GPa (see Fig. 3(a)). Interestingly, the superconducting volume fraction is about the same as compression data, however, the T_c values are not fully recovered. The different T_c between compression and decompression is previously reported in In_2Se_3 , which is intrinsic, as a result of changes in phonon and variation of carrier concentration combined in the pressure quench.³² Further measurements are needed to confirm if there is indeed a suppressed T_c behavior in $\text{Ba}(\text{Fe}_{1-x}\text{Co}_x)_2\text{As}_2$ during decompression, which is beyond the scope of this work.

Figure 4 shows the temperature vs. pressure ($T - P$) phase diagram of $\text{Ba}(\text{Fe}_{1-x}\text{Co}_x)_2\text{As}_2$ with $x = 0.057$. The structural phase transition temperature (T_s), the SDW antiferromagnetic phase transition temperature T_{sdw} , the superconducting transition temperature T_c and the exponent n in $\rho = \rho_0 + AT^n$ are summarized. With increasing pressure, we observe a suppression of the antiferromagnetic phase whereas, the superconducting transition temperature increases, suggesting competition between the two. T_c reaches a maximum at a critical pressure P_c around 3.5 GPa and decreases with further increase in pressure, forming a dome shape. Around P_c , we observe signature of a non-Fermi liquid namely, n close to 1, often associated with quantum criticality.^{30,33} This is accompanied by the above mentioned change in the superconducting diamagnetism. Together, these experimental findings suggest the presence of a QCP at P_c , where T_c is maximum.

Earlier NMR measurements in $\text{Ba}(\text{Fe}_{1-x}\text{Co}_x)_2\text{As}_2$ revealed that the maximum T_c occurs at the antifer-

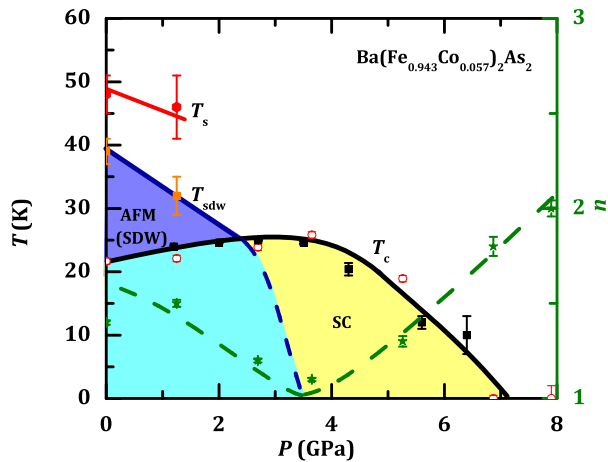


FIG. 4. Temperature - pressure ($T - P$) phase diagram of $\text{Ba}(\text{Fe}_{1-x}\text{Co}_x)_2\text{As}_2$ with $x = 0.057$. The structural phase transition temperature T_s is marked as red hexagon. The SDW phase transition temperature T_{sdw} is marked as orange squares. The superconducting transition temperature T_c is determined from magnetization (solid squares) and resistivity (open circles) measurements. The exponent n is indicated by stars. The light blue and yellow represent the region with large and small superconducting diamagnetism, respectively.

romagnetic QCP possibly due to magnetically mediated superconductivity.³⁴ Such a superconducting pairing mechanism may be applicable in several strongly correlated superconducting systems, where fundamental physical quantities, including the superconducting condensation energy, quasiparticle lifetime, and superfluid

density show abrupt changes at a QCP.³⁵ Hence, the observation of a linear temperature dependence of resistivity at P_c about 3.5 GPa and a possible change in the superconducting volume fraction, may be associated with a quantum phase transition.

D. Conclusions

In summary, electrical resistivity and magnetization under pressure were measured in $\text{Ba}(\text{Fe}_{1-x}\text{Co}_x)_2\text{As}_2$ with $x = 0.057$. Resistivity shows linear temperature dependence around a critical pressure of 3.5 GPa where T_c is maximum. Furthermore, we detected signs of an accompanied change in the superconducting volume. These results are most likely due to a possible pressure tuned QCP hidden inside the superconducting dome of $\text{Ba}(\text{Fe}_{1-x}\text{Co}_x)_2\text{As}_2$.

E. Acknowledgments

Work at HPSTAR was supported by NSAF, Grant No. U1530402. Work at SIMIT was supported by the support of NSFC, Grant No. 11574338. Work at the Ames Laboratory was supported by the U.S. Department of Energy, Basic Energy Sciences under Contract No. DE-AC02-07CH11358. The work in Singapore was supported by the National Research Foundation C NRF Investigatorship (Reference No. NRF-NRFI2015-04). The work at KSU was supported by the National Science Foundation under grant No. DMR-1505826.

* hong.xiao@hpstar.ac.cn † thu@mail.sim.ac.cn

¹ G. R. Stewart, *Rev. Mod. Phys.* **83**, 1589 (2011).

² N. Ni, M. E. Tillman, J.-Q. Yan, A. Kracher, S. T. Hannahs, S. L. Bud'ko, and P. C. Canfield, *Phys. Rev. B* **78**, 214515 (2008).

³ E. Colombier, S. L. Bud'ko, N. Ni, and P. C. Canfield, *Phys. Rev. B* **79**, 224518 (2009).

⁴ P. C. Canfield and S. L. Bud'ko, *Annual Review of Condensed Matter Physics* **1**, 27 (2010), <https://doi.org/10.1146/annurev-conmatphys-070909-104041>.

⁵ N. Ni, A. Thaler, J. Q. Yan, A. Kracher, E. Colombier, S. L. Bud'ko, P. C. Canfield, and S. T. Hannahs, *Phys. Rev. B* **82**, 024519 (2010).

⁶ H. Luo, R. Zhang, M. Laver, Z. Yamani, M. Wang, X. Lu, M. Wang, Y. Chen, S. Li, S. Chang, J. W. Lynn, and P. Dai, *Phys. Rev. Lett.* **108**, 247002 (2012).

⁷ K. Hashimoto, K. Cho, T. Shibauchi, S. Kasahara, Y. Mizukami, R. Katsumata, Y. Tsuruhara, T. Terashima, H. Ikeda, M. A. Tanatar, H. Kitano, N. Salovich, R. W. Giannetta, P. Walmsley, A. Carrington, R. Prozorov, and Y. Matsuda, *Science* **336**, 1554 (2012).

⁸ P. C. Canfield, S. L. Bud'ko, N. Ni, J. Q. Yan, and A. Kracher, *Phys. Rev. B* **80**, 060501 (2009).

⁹ N. Ni, A. Thaler, A. Kracher, J. Q. Yan, S. L. Bud'ko, and P. C. Canfield, *Phys. Rev. B* **80**, 024511 (2009).

¹⁰ J.-H. Chu, J. G. Analytis, C. Kucharczyk, and I. R. Fisher, *Phys. Rev. B* **79**, 014506 (2009).

¹¹ C. Lester, J.-H. Chu, J. G. Analytis, S. C. Capelli, A. S. Erickson, C. L. Condon, M. F. Toney, I. R. Fisher, and S. M. Hayden, *Phys. Rev. B* **79**, 144523 (2009).

¹² X. Y. Huang, Y. P. Singh, D. J. Haney, T. Hu, H. Xiao, H.-H. Wen, S. Zhang, M. Dzero, and C. C. Almasan, *Phys. Rev. B* **96**, 094509 (2017).

¹³ K. Iida, V. Grinenko, F. Kurth, A. Ichinose, I. Tsukada, E. Ahrens, A. Pukenas, P. Chekhonin, W. Skrotzki, A. Teresiak, R. Hhne, S. Aswartham, S. Wurmehl, I. Mnch, M. Erbe, J. Hnisch, B. Holzapfel, S.-L. Drechsler, and D. V. Efremov, *Scientific Reports* **6**, 28390 (2016).

¹⁴ C. Meingast, F. Hardy, R. Heid, P. Adelman, A. Böhrer, P. Burger, D. Ernst, R. Fromknecht, P. Schweiss, and T. Wolf, *Phys. Rev. Lett.* **108**, 177004 (2012).

¹⁵ F. L. Ning, M. Fu, D. A. Torchetti, T. Imai, A. S. Sefat, P. Cheng, B. Shen, and H.-H. Wen, *Phys. Rev. B* **89**, 214511 (2014).

¹⁶ X. Y. Huang, D. J. Haney, Y. P. Singh, T. Hu, H. Xiao, H.-H. Wen, M. Dzero, and C. C. Almasan, *Phys. Rev. B*

- 318 **95**, 184513 (2017).
 319 ¹⁷ S. Arsenijević, H. Hodovanets, R. Gaál, L. Forró, S. L.
 320 Bud'ko, and P. C. Canfield, *Phys. Rev. B* **87**, 224508
 321 (2013).
 322 ¹⁸ S. Sachdev, *Physica Status Solidi* **247**, 537C543 (2010).
 323 ¹⁹ A. S. Sefat, *Reports on Progress in Physics* **74**, 124502
 324 (2011).
 325 ²⁰ K. Ahilan, F. L. Ning, T. Imai, A. S. Sefat, M. A. McGuire,
 326 B. C. Sales, and D. Mandrus, *Phys. Rev. B* **79**, 214520
 327 (2009).
 328 ²¹ K. Ahilan, J. Balasubramaniam, F. L. Ning, T. Imai, A. S.
 329 Sefat, R. Jin, M. A. McGuire, B. C. Sales, and D. Man-
 330 drus, *Journal of Physics: Condensed Matter* **20**, 472201
 331 (2008).
 332 ²² E. Colombier, M. S. Torikachvili, N. Ni, A. Thaler, S. L.
 333 Budko, and P. C. Canfield, *Superconductor Science and*
 334 *Technology* **23**, 054003 (2010).
 335 ²³ V. A. Sidorov, M. Nicklas, P. G. Pagliuso, J. L. Sarrao,
 336 Y. Bang, A. V. Balatsky, and J. D. Thompson, *Phys.*
 337 *Rev. Lett.* **89**, 157004 (2002).
 338 ²⁴ R. Zhou, Z. Li, J. Yang, D. L. Sun, C. T. Lin, and G.-q.
 339 Zheng, *Phys. Rev. B* **87**, 2265 (2013).
 340 ²⁵ S. R. Saha, N. P. Butch, K. Kirshenbaum, and J. Paglione,
 341 *Phys. Rev. B* **79**, 224519 (2009).
 342 ²⁶ S. R. Saha, N. P. Butch, T. Drye, J. Magill, S. Ziemak,
 343 K. Kirshenbaum, P. Y. Zavalij, J. W. Lynn, and
 344 J. Paglione, *Phys. Rev. B* **85**, 024525 (2012).
 345 ²⁷ K. Kudo, K. Iba, M. Takasuga, Y. Kitahama, J.-i. Mat-
 346 sumura, M. Danura, Y. Nogami, and M. Nohara, *Scientific*
 347 *Reports* **3**, 1478 (2013).
 348 ²⁸ P. L. Alireza, Y. T. C. Ko, J. Gillett, C. M. Petrone, J. M.
 349 Cole, G. G. Lonzarich, and S. E. Sebastian, *Journal of*
 350 *Physics: Condensed Matter* **21**, 012208 (2009).
 351 ²⁹ H. Takagi, R. J. Cava, M. Marezio, B. Batlogg, J. J. Kra-
 352 jewski, W. F. Peck, P. Bordet, and D. E. Cox, *Phys. Rev.*
 353 *Lett.* **68**, 3777 (1992).
 354 ³⁰ R. A. Cooper, Y. Wang, B. Vignolle, O. J. Lipscombe,
 355 S. M. Hayden, Y. Tanabe, T. Adachi, Y. Koike, M. Nohara,
 356 H. Takagi, C. Proust, and N. E. Hussey, *Science* **323**, 603
 357 (2009).
 358 ³¹ S. Seo, X. Lu, J.-X. Zhu, R. R. Urbano, N. Curro, E. D.
 359 Bauer, V. A. Sidorov, L. D. Pham, T. Park, Z. Fisk, and
 360 J. D. Thompson, *Nature Physics* **10**, 120 (2013).
 361 ³² F. Ke, H. Dong, Y. Chen, J. Zhang, C. Liu, J. Zhang,
 362 Y. Gan, Y. Han, Z. Chen, C. Gao, J. Wen, W. Yang, X.-J.
 363 Chen, V. V. Struzhkin, H.-K. Mao, and B. Chen, *Ad-*
 364 *vanced Materials* **29**, 1701983 (2017), 1701983.
 365 ³³ P. Gegenwart, Q. Si, and F. Steglich, *Nat Phys* **4**, 186
 366 (2008).
 367 ³⁴ Y. Nakai, T. Iye, S. Kitagawa, K. Ishida, S. Kasahara,
 368 T. Shibauchi, Y. Matsuda, H. Ikeda, and T. Terashima,
 369 *Phys. Rev. B* **87**, 174507 (2013).
 370 ³⁵ C. Panagopoulos, J. L. Tallon, B. D. Rainford, T. Xiang,
 371 J. R. Cooper, and C. A. Scott, *Phys. Rev. B* **66**, 064501
 372 (2002).